



Regulation of brain endothelial cells migration and angiogenesis by P-glycoprotein/caveolin-1 interaction

Stéphane Barakat^{a,b}, Sandra Turcotte^a, Michel Demeule^c, Marie-Paule Lachambre^a, Anthony Régina^a, Loris G. Baggetto^b, Richard Béliveau^{a,*}

^a *Département de Chimie-Biochimie, Laboratoire de Médecine Moléculaire, Université du Québec à Montréal, CP 8888, Succursale Centre-Ville, Montréal, QC, Canada H3C 3P8*

^b *Laboratoire Thérapie Transcriptionnelle Des Cellules Cancéreuses, Institut de Biologie et Chimie des Protéines, Lyon, France*

^c *Angiochem, 201 President Kennedy Avenue (PK-R210), Montreal, QC, Canada H2X 3Y7*

ARTICLE INFO

Article history:

Received 1 May 2008

Available online 15 May 2008

Keywords:

P-glycoprotein
Caveolin-1
Endothelial cells
Migration
Blood–brain barrier
Tubulogenesis
Caveolae

ABSTRACT

We have investigated the involvement of P-glycoprotein (P-gp)/caveolin-1 interaction in the regulation of brain endothelial cells (EC) migration and tubulogenesis. P-gp overexpression in MDCK-MDR cells was correlated with enhanced cell migration whereas treatment with P-gp inhibitors CsA or PSC833 reduced it. Transfection of RBE4 rat brain endothelial cells with mutated versions of MDR1, in the caveolin-1 interaction motif, decreased the interaction between P-gp and caveolin-1, enhanced P-gp transport activity and cell migration. Moreover, down-regulation of caveolin-1 in RBE4 cells by siRNA against caveolin-1 stimulated cell migration. Interestingly, the inhibition of P-gp/caveolin-1 interaction increased also EC tubulogenesis. Furthermore, decrease of P-gp expression by siRNA inhibited EC tubulogenesis. These data indicate that the level of P-gp/caveolin-1 interaction can modulate brain endothelial angiogenesis and P-gp dependent cell migration.

© 2008 Elsevier Inc. All rights reserved.

P-glycoprotein (P-gp) belongs to the ABC (ATP Binding Cassette) transporter superfamily and is responsible for the expulsion of a variety of anti-cancer agents from cancer cells [1]. P-gp is also normally expressed in tissues such as liver, kidney, lung, and the blood–brain barrier (BBB) in order to maintain their physiological function. At the BBB, P-glycoprotein is located at the luminal surface of brain capillaries and is implicated not only in protection from toxic compounds [2] but also as an efflux pump removing pharmacological agents from the brain [3]. Thus, brain permeability is highly regulated by the presence of this transporter. Many functions have been ascribed to P-gp [4]. One of them concerns a role in the membrane translocation of lipids, such as cholesterol and sphingomyelin, from the inner to the outer leaflet [5,6].

One population of P-gp is localized in caveolae, a cholesterol- and sphingomyelin-enriched microdomain [7], and is able to interact with the caveolin scaffolding domain of caveolin-1, a caveolar-specific marker, through a particular domain located

between amino acids 36 and amino acid 44 of P-gp [8,9]. In brain endothelial cells, we have shown that a portion of P-gp molecules is localized in caveolae and interacts with caveolin-1. The interaction between these two proteins inhibits P-gp transport activity [9]. However, the localization of P-gp in caveolae and its interaction with caveolin-1 remains controversial [10,11]. The location of P-gp and its interaction with caveolin-1 could depend on the specific cell line and detergent used in caveolae purification methods [12]. It has also been suggested that P-gp might play a role in dendritic cell migration [13]. Recently, it has been shown that the interaction between P-gp and CD44 contributes towards enhancing the migration and invasion of cancer cells [14].

Caveolin-1, a major protein component of caveolae and an integral membrane protein, is characterized by an unusual hairpin-like conformation in which the N- and C-terminal regions both face the cytosol [15]. Caveolin-1 interacts with many proteins and regulates different signaling pathways critical for diverse cellular function [16,17]. It has been shown that downregulation of caveolin-1 decreased cell migration by activation of ERK [18].

We demonstrate here the existence of P-gp-dependent cell migration and tubulogenesis regulated by caveolin-1. We also investigated the impact of P-gp/caveolin-1 interaction on the migration and tubulogenesis of brain ECs. We evidence the role of P-gp in EC tubulogenesis by using siRNA against MDR1. Finally,

Abbreviations: BCA, bicinchoninic acid; Cav, caveolin; CsA, cyclosporin A; MACS, magnetic cell sorting; ID, immunodetection; IP, immunoprecipitation; MDCK, Madin-Darby canine kidney cells; MDR, multidrug resistance; P-gp, P-glycoprotein; PVDF, polyvinylidene difluoride; TBS, Tris-buffered saline; TBS-T, Tris-buffered saline containing 0.1% Tween 20; ECM, extracellular matrix; ECs, endothelial cells.

* Corresponding author. Fax: +1 514 987 0246.

E-mail address: oncomol@nobel.si.uqam.ca (R. Béliveau).

using siRNA against caveolin-1, we tested the impact of caveolin-1 downregulation on P-gp-dependent brain EC migration.

Materials and methods

Materials. DMEM (high glucose), RPMI 1640, α -MEM and F-12 media were purchased from Gibco-BRL Life Technologies, Inc. (Burlington, ON, Canada). Hoechst 33342 was obtained from Sigma Chemical Co. (St. Louis, MO). Fetal bovine serum (FBS) was obtained from HyClone (Logan, UT). Goat anti-PECAM-1 antibody, used in Western blotting analysis, was from Santa Cruz Biotechnology (Santa Cruz, CA) and cross-reacts with rat PECAM-1 according to the manufacturer's product information. A mAb directed against endothelial nitric oxide synthase (eNOS; Transduction Laboratories, Mississauga, ON, Canada) was raised against the C-terminal portion of the protein and cross-reacts against the human, rat and mouse orthologues. FuGENE and PVDF were purchased from Roche Molecular Biochemicals (QC, Canada). Antibodies directed against caveolin-1 (mAb or pAb) and P-gp (mAb C219) were purchased from BD Transduction Laboratories (Lexington, KY) and ID Labs (London, ON, Canada), respectively. Anti-mouse and anti-goat IgG, linked to horseradish peroxidase, were purchased from Jackson ImmunoResearch Laboratories (West Grove, PA) and enhanced Chemiluminescence Reagent Plus (ECL) reagents were from NENTM Life Science Products (Boston, MA). Cyclosporin A and SDZ PSC833 were provided by Novartis Pharma Canada Inc. (Dorval, QC, Canada). Protein G-Sepharose beads were purchased from Amersham Pharmacia Biotech (Uppsala, Sweden). Hiperfect and HP-validated human caveolin-1 siRNA (1027400) and MDR1 siRNA (SI01994055) were obtained from Qiagen (Mississauga, ON, Canada). Other biochemical reagents were from Sigma (Oakville, ON).

Cell culture and experimental conditions. RBE4 immortalized rat brain microvessel ECs were a gift from Françoise Roux (INSERM, Paris, France) and were grown as previously described [19]. Non-transfected MDCK and MDR1-transfected MDCK cells were gifts from Amanda Yancy (AstraZeneca Pharmaceuticals, LP) and were maintained in DMEM high glucose medium containing 10% heat-inactivated FBS. Cells were cultured at 37 °C in a humidified atmosphere of 5% CO₂.

Transfection with P-gp mutants. RBE4 cells were seeded in 6-well plates or in 60-mm culture plates. After 24 h, the cells were transiently transfected, in serum-free medium, with FuGENE 6 transfection reagent using 1 or 2 μ g of DNA (either WT, YWAA or F37A). Five hours post-transfection, the culture medium was replaced with fresh complete medium and cells were used 48 h after transfection.

Transfection of siRNA against caveolin-1 and MDR1. RBE4 cells were seeded in 6-well plates or in 60-mm culture plates. The cells were transiently transfected, in serum-free medium, with Hiperfect transfection reagent using 50 nM siRNA against caveolin-1 or MDR1 in 6-well plates or in 60-mm culture plates. Cells were used 48 h after transfection.

Hoechst 33342 accumulation. Transfected cells in 6-well plates were incubated at 37 °C with 20 μ M Hoechst 33342 (bisbenzimidazole) in serum-free medium. The fluorescence of the intracellular dye was monitored continuously using a spectrofluorometer (Spectra-Max Gemini, Molecular Devices, Sunnyvale, CA, USA) at wavelengths of 355 nm for excitation and 460 nm for emission.

Western blot analysis. MDCK-MDR1, MDCK-WT, and RBE4 cells were washed twice with phosphate buffered saline (PBS) and lysed in buffer containing 50 mM Tris-HCl, pH 7.5, 150 mM NaCl, 0.1% SDS, 1% NP-40, 0.5% deoxycholate, and protease inhibitors for 30 min at 4 °C. Proteins in cell lysates were quantified by the micro BCA method. Cell lysates were solubilized with Laemmli buffer and heated (caveolin-1), or not (P-gp), for 4 min at 95 °C. Proteins were

separated by polyacrylamide gel electrophoresis in the presence of SDS (SDS-PAGE), followed by semi-dry transfer onto polyvinylidene difluoride membranes (PVDF) using standard procedures. Immunodetection of caveolin-1 and P-gp was performed with specific antibodies. Horseradish peroxidase (HRP)-conjugated anti-IgG antibodies were used as secondary antibodies, and antigens were detected using Western blot Chemiluminescence Reagent Plus. Blots were exposed to Fuji films and the autoradiograms were scanned with a Chemilmager (Alpha Innotech Corporation, San Leandro, CA).

Cell migration assay. Migration of cells was carried out on collagen-coated Transwell filters (8- μ m-pore-size polycarbonate filters; Costar). 60,000 cells were seeded on top of the filter in a final volume of 200 μ l in serum-free medium. In the lower chamber, 500 μ l of medium containing serum was used as chemoattractant. After 30 min, 5 μ M cyclosporin A or PSC833 was added to both the lower and upper chambers. After overnight incubation at 37 °C and 5% CO₂, cells were fixed in 3.7% formaldehyde, stained with crystal violet for 30 min, and washed with water. Cells in the top well were removed by swiping with cotton swabs and migration was determined by counting the cells on the underside of the membrane. Migrating cells were visualized at 100 \times magnification using a digital Nikon CoolpixTM 5000 camera attached to a Nikon TMS-F microscope and the average number of migrated cells per field was assessed by counting at least five random fields per filter using Northern Eclipse software (Empix Imaging, Mississauga, ON).

Capillary-like structure formation assay on collagen. Induction of RBE4 tube formation was performed by mixing 8 volumes cold collagen solution (type 1) with 1 volume 10 \times MEM and 1 volume sodium bicarbonate (22 mg/ml). The gel was polymerized by incubation at 37 °C for 10 min. About 40,000 cells were seeded onto collagen gel for 24 h to obtain a subconfluent monolayer. Then, the culture medium was removed and another layer of collagen gel was added on top of the first gel and polymerized for 10 min at 37 °C. Culture medium (1 ml) was added and tube formation was evaluated after 2–3 days. Tubular structures were visualized at a 40 \times magnification using a digital Nikon CoolpixTM 5000 camera attached to a Nikon TMS-F microscope and Northern Eclipse Software.

Capillary-like structure formation assay on matrigel. Matrigel (12.5 mg/ml) was thawed at 4 °C, and 50 μ l were quickly added to each well of a 96-well plate and allowed to solidify for 30 min at 37 °C. The wells were then incubated for 12 h at 37 °C with RBE4 (50,000 cells/well). After incubation, tubular structures were visualized at described above.

Data analysis. Statistical analyses were made with Student's paired *t*-test using GraphPad Prism (San Diego, USA). Significance was assumed for *P* values less than 0.05.

Results

Identification of P-gp dependent migration

P-gp and caveolin-1 were detected in the MDCK-WT and -MDR1 cell lines by Western blot (Fig. 1A). P-gp was highly expressed in MDCK-MDR1 in comparison to the MDCK-WT cell line. In contrast, caveolin-1 levels were similar in both cell lines. Hoechst dye accumulation was measured in both MDCK-WT and -MDR1 cells (Fig. 1B). P-gp overexpression in MDCK-MDR1 cells caused a significant, 50% reduction in dye accumulation.

Migration of MDCK-WT and MDCK-MDR1 cells was measured in the presence or absence of the specific P-gp inhibitors cyclosporin A and PSC833 in order to determine the involvement of P-gp in cell migration (Fig. 1C). In absence of inhibitors, MDCK-MDR1 cells migration was 3-fold higher than that of MDCK-WT cells. In presence of P-gp inhibitors, MDCK-MDR1 cells migration

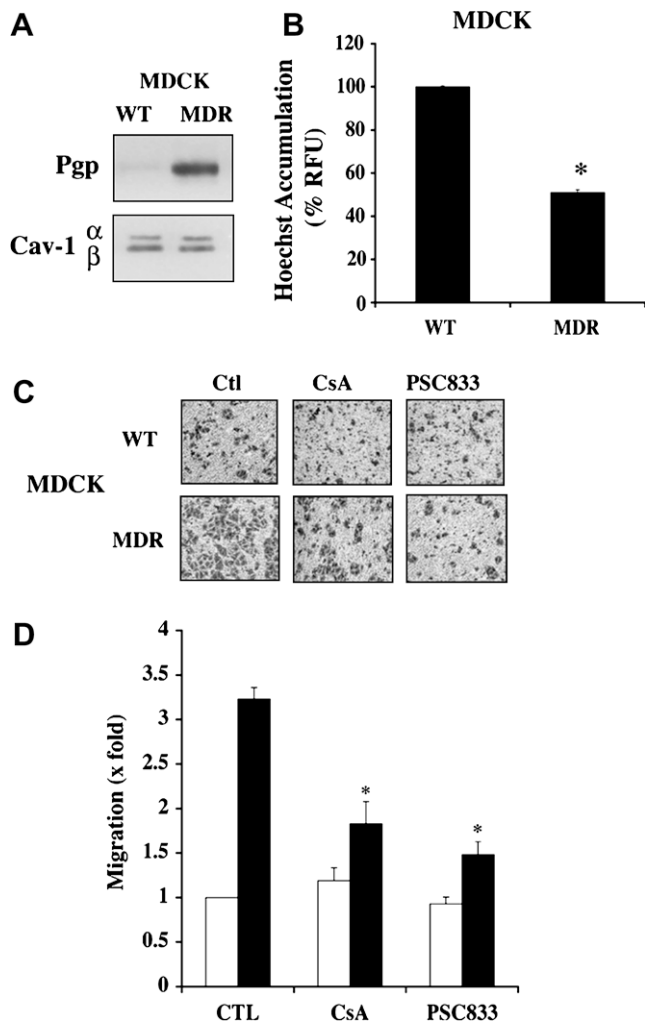


Fig. 1. Correlation between P-gp expression, transport activity and cell migration in MDCK-WT and -MDR1 cells. (A) P-gp and caveolin-1 detection in MDCK-WT and -MDR cells. About 10 μ g of total proteins were separated by 8% and 12.5% SDS-PAGE, respectively, followed by immunoblot using C219 anti-P-gp mAb and anti-caveolin-1 mAb. (B) MDCK-WT and -MDR1 were incubated with 20 μ M Hoechst 33342 in serum-free medium at 37 $^{\circ}$ C for one hour. Fluorescence was measured continuously at 355 nm and 460 nm for excitation and emission, respectively. The results were expressed as the percentage of Hoechst dye accumulation compared to the MDCK-WT cells. (C) Migration was performed on collagen after overnight incubation at 37 $^{\circ}$ C of cells treated (or not) with CsA or PSC833. The levels of cell migration were quantified. White and black bars represent, respectively, MDCK-WT and MDR1 cell migration. Data represent means \pm SD of results obtained from three different experiments performed in triplicate. Asterisks indicate statistical significance (p value < 0.05, Student's t -test).

was significantly reduced whereas MDCK-WT cells migration was unchanged.

Caveolin-1/P-gp interaction regulates P-gp activity inhibit cells migration

P-gp transport activity was investigated in caveolin-1 siRNA transfected RBE4 cells. Forty-eight hours post-transfection, caveolin-1 and P-gp were detected in ECs (Fig. 2A). Caveolin-1 was down-regulated by 90% compared to the control, as determined by densitometry analysis (data not shown), whereas P-gp expression was unchanged. Hoechst 33342 accumulation was measured in siRNA caveolin-1 transfected RBE4 cells (Fig. 2B). Hoechst dye accumulation in transfected cells was decreased after 1 h by 40% compared to the control.

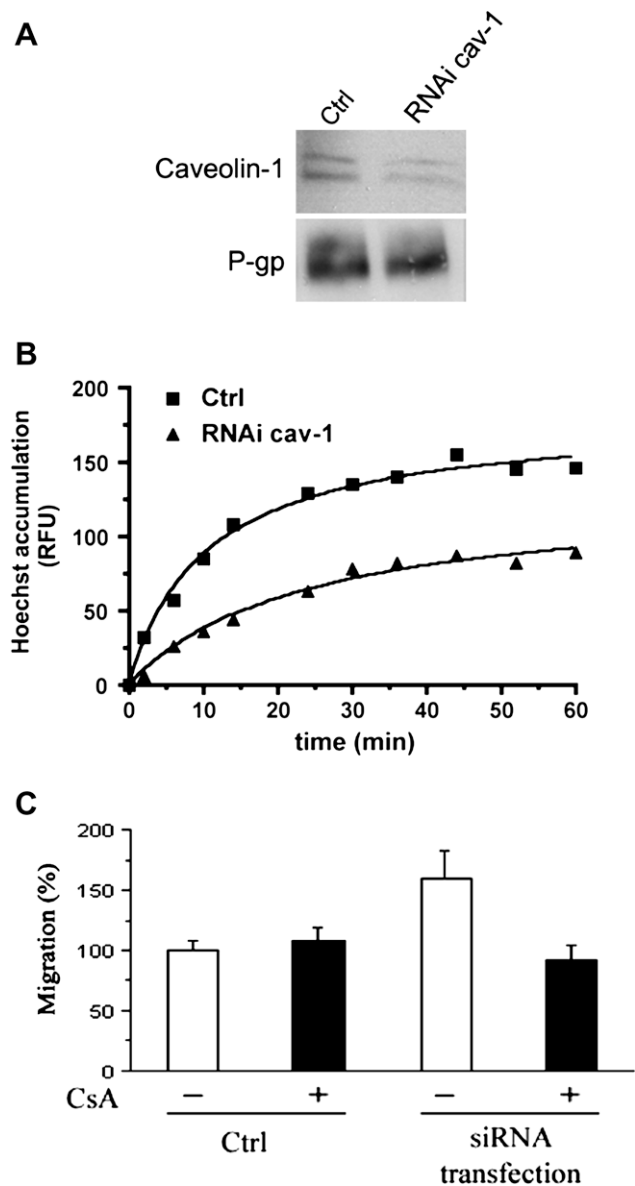


Fig. 2. Caveolin-1 downregulation by siRNA and modulation of P-gp transport activity. (A) RNAi against caveolin-1 was transfected using Hiperfect transfection reagent in RBE4 endothelial cells. About 48 h post-transfection, caveolin-1 and P-gp were detected by immunoblot. One representative experiment of three is shown. (B) RBE4 cells were incubated with 20 μ M Hoechst 33342 in serum-free medium at 37 $^{\circ}$ C for one hour. Fluorescence was measured continuously at 355 nm and 460 nm for excitation and emission, respectively. The results are expressed in relative fluorescence units (RFU). Data represent means \pm SD of results obtained from three different experiments performed in triplicate. (C) Migration was performed after seeding control and siRNA transfected RBE4 cells onto collagen-coated filters. Cells were incubated overnight at 37 $^{\circ}$ C and 5% CO₂. Migration was measured using the Eclipse software as described under Materials and methods. The results were expressed as the percentage of cell migration compared to control cells. Data represents the means \pm SD of results obtained from three experiments performed in triplicate. Asterisk represents statistical significance (p < 0.05, Student's t -test).

Migration of caveolin-1 siRNA transfected RBE4 cells was evaluated. As shown in Fig. 2C, down-regulation of caveolin-1 resulted in an increase in RBE4 cells migration by 1.5-fold compared to the control cells. Treatment with CsA 5 μ M inhibited the migration of siRNA transfected RBE4 cells. Migration of control cells was unaffected by CsA treatment.

We next measured the impact of P-gp/caveolin-1 interaction on RBE4 cell migration by transfecting these cells with two P-gp encoding MDR1 mutants that had been mutated in the caveolin-

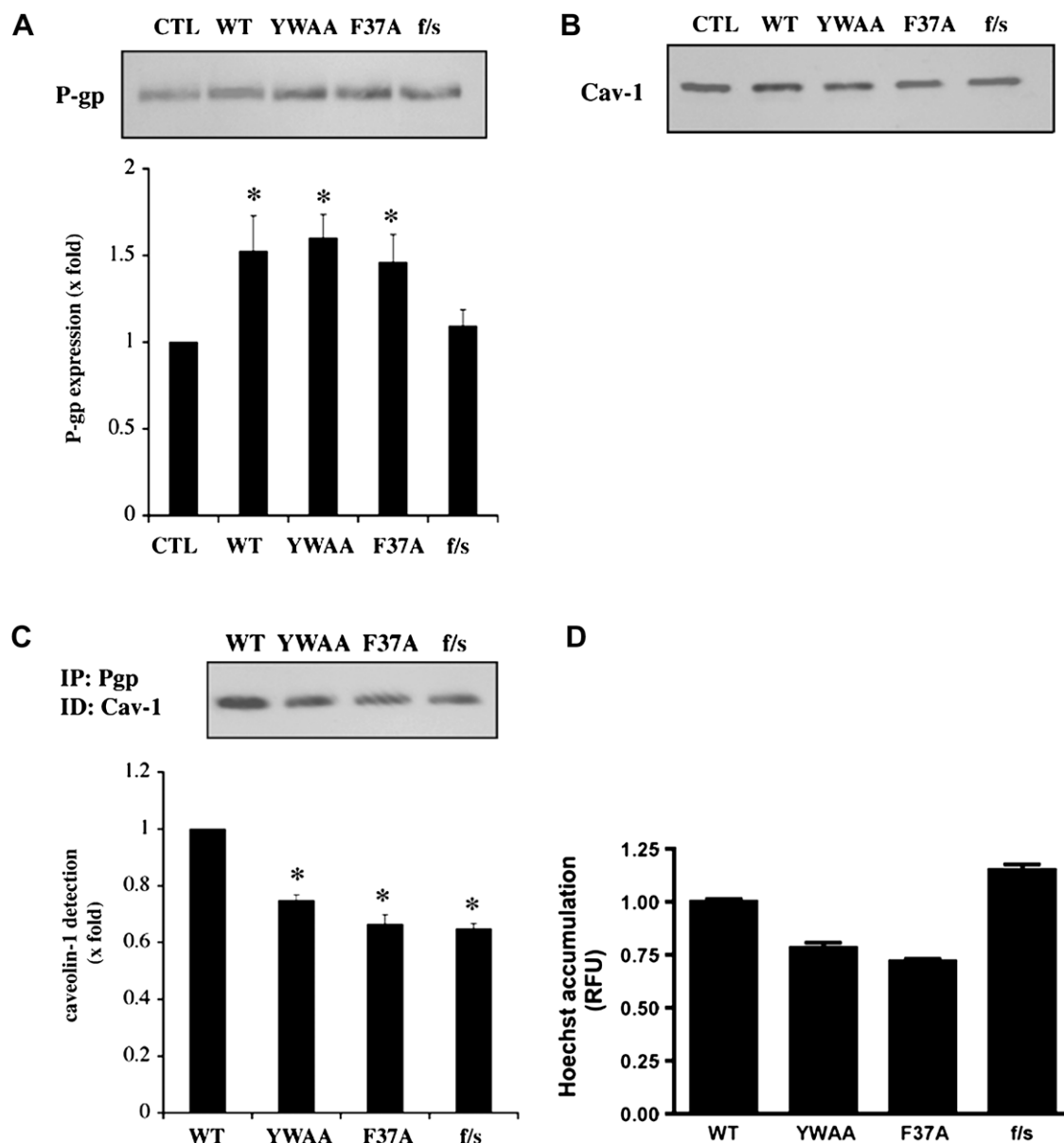


Fig. 3. Effects of transfecting MDR1 wild-type and mutants on P-gp/caveolin-1 interaction. (A) P-gp was detected in transfected RBE4 cells by immunoblot from 10 μ g/ml total protein, as described under Materials and methods. One representative experiment of three separate experiments is shown. P-gp expression was evaluated by densitometry analysis in order to determine transfection efficiency, which was evaluated at around 50% for MDR1 wild-type and mutant coding plasmids. (B) Caveolin-1 was detected as described above for P-gp. (C) P-gp immunoprecipitation from 200 μ g/ml RBE4 transfected cell lysates was performed as described under Materials and methods. Caveolin-1 was identified by immunoblot. Caveolin-1 binding levels were determined by densitometry analysis. Asterisks indicate statistical significance of the three independent experiments ($p < 0.05$, Student's *t*-test). (D) About 48 h post-transfection, RBE4 WT, YWAA, FA and *f/s* transfected cells were incubated with 20 μ M Hoechst 33342 and the fluorescence was followed continuously at 355 nm for excitation and 460 nm for emission. These results correspond to three independent experiments. Asterisks denote statistical significance ($p < 0.05$, Student's *t*-test).

binding motif. The P-gp N-terminal domain contains a caveolin-1-binding motif between amino acid residues 37 and 45 (FSMFRYSNW). In the first P-gp mutant, YWAA, Tyr42 (Y), and Trp45 (W) were replaced with Ala residues. In the other mutant, F37A, Phe37 (F) was replaced with Ala. An additional mutant called frameshift (*f/s*), which contains a deletion in the translational start codon, was used as a negative control.

P-gp was detected in cells transfected with wild-type or mutated MDR1 using the C219 mAb (Fig. 3A). Densitometric analysis of the Western blot showed a 1.5-fold increase in P-gp expression in cells transfected with WT or MDR1 mutants compared to control cells. Caveolin-1 was also detected by Western blot. Caveolin-1 expression was similar in control cells or cells transfected with

wild-type or MDR1 mutants (Fig. 3B). We next immunoprecipitated P-gp and detected caveolin-1 by Western blot. Fig. 3C shows that transfection of wild-type MDR1 led to an increase in P-gp/caveolin-1 interaction by 40% compared to the control *f/s* cells, as determined by densitometry analysis. The interaction between caveolin-1 and P-gp was lower in RBE4 cells transfected with mutated MDR1 than with wild-type MDR1. The caveolin-1/P-gp interaction was reduced by 25 and 35%, respectively, for the YWAA and F37A mutations (Fig. 3C). Hoechst dye accumulation was decreased by similar amounts 22 and 28%, respectively, for the YWAA and F37A mutant transfected cells compared to the wild-type-transfected cells (Fig. 3D). Thus, caveolin-1 interaction with P-gp is able to inhibit P-gp transport activity whereas mutations in

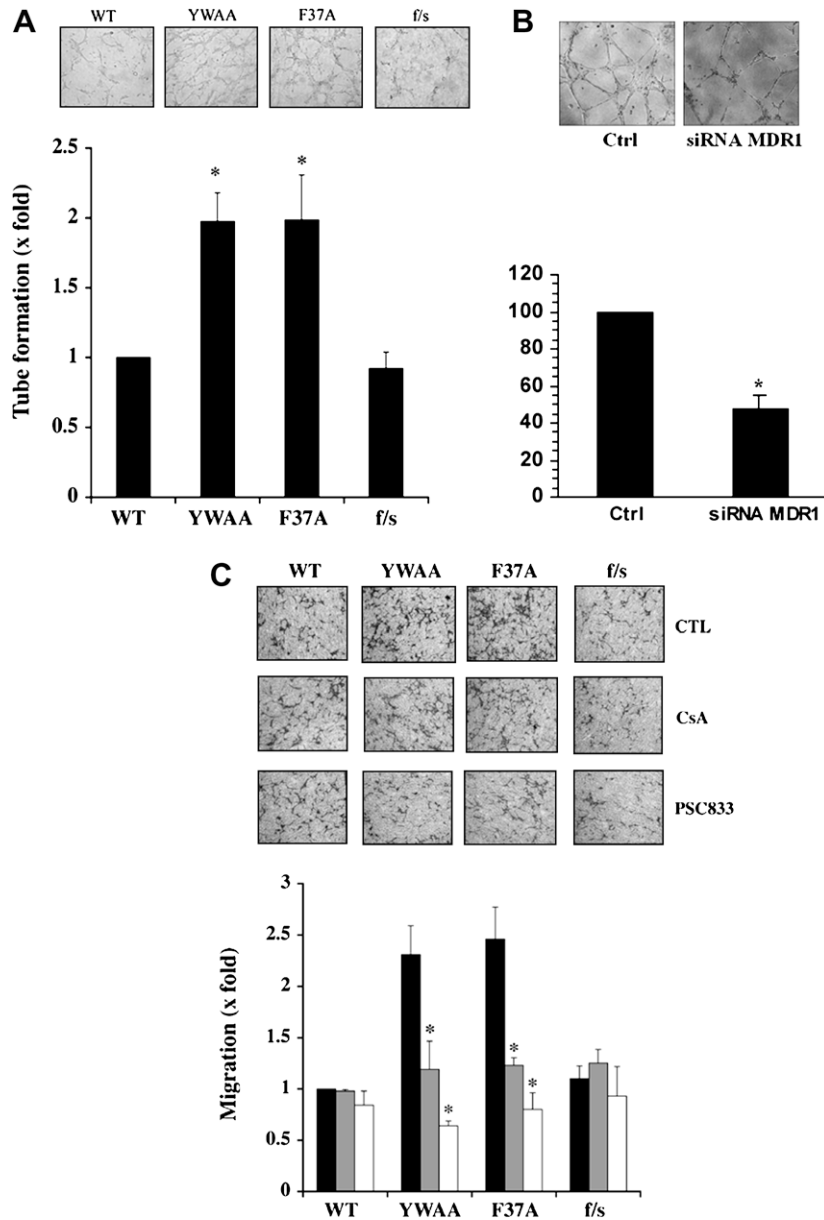


Fig. 4. Mutations of the caveolin-1 binding site of P-gp affect EC tubulogenesis and migration. (A) Tubulogenesis of RBE4 cells transfected with wild-type or mutant MDR1 coding plasmids was assessed on collagen gel after overnight incubation at 37 °C. Tube formation and the length of tubular-like structures were evaluated after 2–3 days using microscopy at 10× magnification. Length of tubular-like structures was measured using the Eclipse Software. (B) Tubulogenesis of RBE4 cells transfected with siRNA directed against *mdr1a* (rat) and tube formation performed on Matrigel. Image and tube length were evaluated as described previously. Data represent means ± SD of results obtained from three different experiments performed in triplicate (* indicate p value < 0.05, Student's t -test). (C) Migration of RBE4 cells transfected with wild-type or mutant MDR1 coding plasmids was assessed on collagen after overnight incubation at 37 °C. Cells were treated or not with CsA or PSC833 overnight. Photographs of filters were taken with a digital Nikon Coolpix™ 5000 camera attached to a Nikon TMS-F microscope (100×). Quantification of cell migration was performed by counting the cells on the underside of the membrane using Northern Eclipse software. Data represent means ± SD of results obtained from three different experiments performed in triplicate [control (black), CsA (grey), PSC833 (white)]. Asterisks indicate statistical significance (p value < 0.05, Student's t -test).

the caveolin-1 interaction motif of P-gp enhance its transport activity in ECs. These data strongly indicate that caveolin-1 regulates P-gp activity in these rat brain ECs.

Involvement of caveolin-1/P-gp interaction in tubulogenesis

RBE4 cells transfected with either mutant or wild-type MDR1 were grown on a matrix of collagen. An enhanced capillary-like network was observed for mutants MDR1 transfected RBE4 cells (Fig. 4A). The length of the capillary-like structure was similar in the control *f/s* and wild-type MDR1 transfected cells. However, in the case of the mutants YWAA and F37A, the length of the capil-

lary-like tubular structure was increased by about 75% compared to the wild-type MDR1 transfected cells. RBE4 cells were then transfected with siRNA directed against MDR1 in order to precise if tubulogenesis was P-gp dependent. Forty-eight hours post-transfection, P-gp was detected by immunoblotting and densitometric analysis was performed. A 40% decrease of P-gp expression was measured (data not shown). siRNA MDR1 transfected RBE4 cells were grown in collagen matrix. The capillary-like structure formed was visualized by microscopy and analyzed using Eclipse Software (Fig. 4B). Results show that siRNA-associated diminution of P-gp expression was correlated with a reduction in tubular-like structure formation by 54% compared to the control cells. We next mea-

sured migration of the transfected RBE4 cells using modified Boyden chambers. Cells were seeded on the top of the filter coated with collagen and medium-containing serum was used as chemo-attractant. As previously, we measured cell migration overnight in the presence or absence of the P-gp inhibitors CsA or PSC833 (Fig. 4C). Rate of cell migration was similar between cells expressing wild-type MDR1 or the control f/s in the presence or absence of CsA or PSC833. However, the migration of cells transfected with either YWAA or F37A MDR1 was increased by 75% compared to the wild-type MDR1 transfected cells. The addition of 5 μ M CsA or PSC833 inhibited the migration of cells transfected with mutant MDR1. In fact, in the presence of both P-gp inhibitors, migration was similar for cells expressing wild type or mutated P-gp.

Discussion

In this study, we have shown that the increased migration of MDCK-MDR1 cells was associated with P-gp overexpression, in agreement with previous studies [14,20]. Disruption of the *mdr1a* allele in mice induced a significant decrease in cell migration [21]. Another study demonstrated that P-gp regulates dendritic cell migration to afferent lymphatic vessels [13]. A recent work has shown that P-gp and CD44 colocalization was associated with cell invasion and migration [14]. Here, we are reporting for the first time that P-gp could be involved in the migration of brain capillary endothelial cells and angiogenesis. In parallel, we also provide evidence that reduction of caveolin-1/P-gp interaction stimulates tubulogenesis and migration of BBB endothelial cells.

P-gp is known to act as an efflux pump both of xenobiotics and of endogenous compounds, but it is also able to translocate a wide variety of lipids such as cholesterol, sphingomyelin or ceramide from the inner to the outer membrane leaflet [6]. A few of the compounds transported by P-gp act as signals for EC migration. In particular, the sphingomyelin/ceramide/sphingosine-1-phosphate pathway has been shown to be involved in migration [22]. It has also been proposed that platelet activating factor PAF, which stimulates angiogenesis, is transported by P-gp [23]. New functions for P-gp continue to be discovered, many of those are correlated to lipid transport. In this study, we have shown that mutations of the caveolin-binding motif of P-gp induce a reduction in caveolin-1/P-gp interaction but also stimulate P-gp transport activity. These mutations enhance RBE4 cell migration and tubulogenesis. The use of CsA and PSC833, two P-gp inhibitors, reduced cell migration and allowed us to correlate this mechanism directly to P-gp transport activity.

Caveolin-1, which is downregulated in glioblastomas, is able to interact with and negatively regulate a wide variety of signalling proteins, including some involved in cell migration [24]. Via these functions, caveolin-1 could play an important role in cell movement [25]. Here, we have demonstrated that P-gp is directly involved in cell migration through its transport activity. This particular function is regulated by caveolin-1 through its interaction with P-gp. Downregulation of caveolin-1 stimulates cell migration, which returned to the control values when treated by CsA or PSC833, indicating that ECs migration is P-gp dependent.

We have already established that P-gp and caveolin-1 can interact and that this interaction led to P-gp transport activity inhibition [12]. In this study, we established that mutations in the caveolin-binding motif of P-gp reduced P-gp/caveolin-1 interaction and provoked the stimulation of tubulogenesis. A previous study showed that caveolin-1 was necessary for enhancement of the first step of tubulogenesis [2]. By using siRNA against MDR1, we showed that P-gp participated also to ECs tubulogenesis. Consequently, these results suggest that P-gp could participate in tubulogenesis depending in the interaction with caveolin-1, which

regulated P-gp transport activity. In the case of highly vascularized brain tumors in which caveolin-1 is downregulated, the increase in P-gp transport activity could thus contribute towards increasing the MDR phenotype of these tumors and in angiogenesis.

In conclusion, these are the first results showing that P-gp, in collaboration with caveolin-1, participates in migration and tubulogenesis of brain endothelial cells. Understanding of P-gp activity modulation particularly by caveolin-1 could be useful not only in facilitating the delivery of anti-cancer agents to the brain for treatment of cerebral tumors but also in modulating angiogenesis. Thus, molecular-based therapies modulating P-gp/caveolin-1 interaction may be a new, effective strategy against cerebral tumors and other neurodegenerative diseases.

Acknowledgment

This study was supported by grant from the National Sciences and Engineering Research Council of Canada (NSERC) to R. Béliveau. Dr Béliveau holds a Research Chair in Neurosurgery (Claude-Bertrand) from Centre Hospitalier de l'Université de Montréal.

References

- [1] R.L. Juliano, The role of drug delivery systems in cancer chemotherapy, *Prog. Clin. Biol. Res* 9 (1976) 21–32.
- [2] M. Demeule, A. Regina, J. Jodoin, A. Laplante, C. Dagenais, F. Berthelot, A. Moghrabi, R. Beliveau, Drug transport to the brain: key roles for the efflux pump P-glycoprotein in the blood-brain barrier, *Vascul. Pharmacol.* 38 (2002) 339–348.
- [3] J.W. Jonker, E. Wagenaar, L. van Deemter, R. Gottschlich, H.M. Bender, J. Dasenbrock, A.H. Schinkel, Role of blood-brain barrier P-glycoprotein in limiting brain accumulation and sedative side-effects of asimadoline, a peripherally acting analgesic drug, *Br. J. Pharmacol.* 127 (1999) 43–50.
- [4] R.W. Johnstone, A.A. Ruefli, M.J. Smyth, Multiple physiological functions for multidrug transporter P-glycoprotein?, *Trends Biochem. Sci.* 25 (2000) 1–6.
- [5] P. Debry, E.A. Nash, D.W. Neklason, J.E. Metherall, Role of multidrug resistance P-glycoproteins in cholesterol esterification, *J. Biol. Chem.* 272 (1997) 1026–1031.
- [6] A. van Helvoort, M.L. Giudici, M. Thielemans, G. van Meer, Transport of sphingomyelin to the cell surface is inhibited by brefeldin A and in mitosis, where C6-NBD-sphingomyelin is translocated across the plasma membrane by a multidrug transporter activity, *J. Cell Sci.* 110 (Pt 1) (1997) 75–83.
- [7] Y. Lavie, G. Fiucci, M. Czarny, M. Liscovitch, Changes in membrane microdomains and caveolae constituents in multidrug-resistant cancer cells, *Lipids* 34 (Suppl) (1999) S57–S63.
- [8] M. Demeule, J. Jodoin, D. Gingras, R. Beliveau, P-glycoprotein is localized in caveolae in resistant cells and in brain capillaries, *FEBS Lett.* 466 (2000) 219–224.
- [9] J. Jodoin, M. Demeule, L. Fenart, R. Cecchelli, S. Farmer, K.J. Linton, C.F. Higgins, R. Beliveau, P-glycoprotein in blood-brain barrier endothelial cells: interaction and oligomerization with caveolins, *J. Neurochem.* 87 (2003) 1010–1023.
- [10] J.W. Hinrichs, K. Klappe, I. Hummel, J.W. Kok, ATP-binding cassette transporters are enriched in non-caveolar detergent-insoluble glycosphingolipid-enriched membrane domains (DIGs) in human multidrug-resistant cancer cells, *J. Biol. Chem.* 279 (2004) 5734–5738.
- [11] G. Radeva, J. Perabo, F.J. Sharom, P-Glycoprotein is localized in intermediate-density membrane microdomains distinct from classical lipid rafts and caveolar domains, *FEBS J.* 272 (2005) 4924–4937.
- [12] K. Gaus, M. Rodriguez, K.R. Ruberu, I. Gelissen, T.M. Sloane, L. Kritharides, W. Jessup, Domain-specific lipid distribution in macrophage plasma membranes, *J. Lipid. Res.* 46 (2005) 1526–1538.
- [13] G.J. Randolph, S. Beaulieu, M. Pope, I. Sugawara, L. Hoffman, R.M. Steinman, W.A. Muller, A physiologic function for P-glycoprotein (MDR-1) during the migration of dendritic cells from skin via afferent lymphatic vessels, *Proc. Natl. Acad. Sci. USA* 95 (1998) 6924–6929.
- [14] K.E. Miletti-Gonzalez, S. Chen, N. Muthukumar, G.N. Saglimbeni, X. Wu, J. Yang, K. Apolito, W.J. Shih, W.N. Hait, L. Rodriguez-Rodriguez, The CD44 receptor interacts with P-glycoprotein to promote cell migration and invasion in cancer, *Cancer Res.* 65 (2005) 6660–6667.
- [15] P. Dupree, R.G. Parton, G. Raposo, T.V. Kurzchalia, K. Simons, Caveolae and sorting in the trans-Golgi network of epithelial cells, *EMBO J.* 12 (1993) 1597–1605.
- [16] A.W. Cohen, B. Razani, X.B. Wang, T.P. Combs, T.M. Williams, P.E. Scherer, M.P. Lisanti, Caveolin-1-deficient mice show insulin resistance and defective insulin receptor protein expression in adipose tissue, *Am. J. Physiol. Cell. Physiol.* 285 (2003) C222–C235.

- [17] A. Uittenbogaard, E.J. Smart, Palmitoylation of caveolin-1 is required for cholesterol binding, chaperone complex formation, and rapid transport of cholesterol to caveolae, *J. Biol. Chem.* 275 (2000) 25595–25599.
- [18] D. Volonte, Y. Liu, F. Galbiati, The modulation of caveolin-1 expression controls satellite cell activation during muscle repair, *FASEB J.* 19 (2005) 237–239.
- [19] F. Roux, O. Durieu-Trautmann, J.M. Bourre, A.D. Strosberg, P.O. Couraud, Immortalized rat brain microvessel endothelial cells: I—expression of blood-brain barrier markers during angiogenesis, *Adv. Exp. Med. Biol.* 331 (1993) 201–204.
- [20] W. Muller, W. Saeger, L. Wellhausen, K.M. Derwahl, C. Hamacher, D.K. Ludecke, Markers of function and proliferation in non-invasive and invasive bi- and plurihormonal adenomas of patients with acromegaly: an immunohistochemical study, *Pathol. Res. Pract.* 195 (1999) 595–603.
- [21] Y. Mochida, K. Taguchi, S. Taniguchi, M. Tsuneyoshi, H. Kuwano, T. Tsuzuki, M. Kuwano, M. Wada, The role of P-glycoprotein in intestinal tumorigenesis: disruption of *mdr1a* suppresses polyp formation in *Apc(Min/+)* mice, *Carcinogenesis* 24 (2003) 1219–1224.
- [22] F. Maupas-Schwalm, N. Auge, C. Robinet, J.P. Cambus, S.J. Parsons, R. Salvayre, A. Negre-Salvayre, The sphingomyelin/ceramide pathway is involved in ERK1/2 phosphorylation, cell proliferation, and uPAR overexpression induced by tissue-type plasminogen activator, *FASEB J.* 18 (2004) 1398–1400.
- [23] R.J. Raggars, I. Vogels, G. van Meer, Multidrug-resistance P-glycoprotein (MDR1) secretes platelet-activating factor, *Biochem. J.* 357 (2001) 859–865.
- [24] Y. Fujita, S. Maruyama, H. Kogo, S. Matsuo, T. Fujimoto, Caveolin-1 in mesangial cells suppresses MAP kinase activation and cell proliferation induced by bFGF and PDGF, *Kidney Int.* 66 (2004) 1794–1804.
- [25] A. Navarro, B. Anand-Apte, M.O. Parat, A role for caveolae in cell migration, *FASEB J.* 18 (2004) 1801–1811.